Available online at www.sciencedirect.com
ScienceDirect
Acta Biomaterialia xxx (2006) xxx–xxx
Acta BIOMATERIALIA
www.actamat-journals.com

Force response and actin remodeling (agglomeration) in fibroblasts due to lateral indentation

Shengyuan Yang, M. Taher A. Saif *

Department of Mechanical and Industrial Engineering, University of Illinois at Urbana-Champaign, 1206 West Green Street, Urbana, IL 61801, USA

Received 18 April 2006; received in revised form 5 July 2006; accepted 26 July 2006

Abstract

We report the loading and unloading force response of single living adherent fibroblasts due to large lateral indentation obtained by a two-component microelectromechanical systems force sensor. Strong hysteretic force response is observed for all the tested cells. For the loading process, the force response is linear (often with small initial non-linearity) to a deformation scale comparable to the undeformed cell size, followed by plastic yielding. In situ visualization of actin fibers by tagging with green fluorescent protein indicates that during the indentation process, actin network possibly decomposes irreversibly at discrete locations where well-defined circular actin agglomerates appear all over the cell, which explains the irreversibility of the force response. Similar agglomeration is observed when the cell is compressed laterally by a micro plate. The distribution pattern of the agglomerates strongly correlates with the arrangement of the actin fibers of the pre-indented cell. The size of the agglomerates increases with time as t^{α}, initially with $\alpha = 2$–3 followed by $\alpha = 0.5$–1. The higher growth rate suggests influx of actin into the agglomerates. The slower rate suggests a diffusive spreading, but the diffusion constant is two orders of magnitude lower than that of an actin monomer through the cytoplasm. Actin agglomeration has previously been observed due to biochemical treatment, gamma-radiation, and ischemic injury, and has been identified as a precursor to cell death. We believe this is the first evidence of actin agglomeration due to mechanical indentation/compression. The study demonstrates that living cells may initiate similar functionalities in response to dissimilar mechanical and biochemical stimuli.

Keywords: Cell mechanics; Large deformation; Microelectromechanical systems (MEMS); Green fluorescent protein (GFP); Actin fibers

1. Introduction

Study of the mechanical behavior of cells has gained considerable attention during the past 10 years [1–3]. The study is motivated by the observation that a wide range of cell functionalities (e.g., motility, growth, and differentiation) are related to mechanical stimuli. Cells undergo mechanical deformations that originate from various sources such as during systolic and diastolic cycles. Large deformations, on the order of cell size, are also common in soft biological tissues during normal functioning [4–6], injuries [7], and during growth on scaffolds [8,9].

Force response of single living fibroblasts subject to large stretches have been measured by microelectromechanical systems (MEMS) force sensors, and the response was found to be strongly linear, reversible and repeatable [10]. Cell response and cytoskeletal reorganization under indentation and compression yet remain mostly unexplored. Indentation may occur during mechanical injuries. Endothelial cells of blood vessels are subjected to cyclic radial compression which may play a role in the damage of endothelium during atherosclerosis.

For this paper, we used a two-component MEMS force sensor to measure the loading and unloading force response of single living fibroblasts subject to lateral indentation where the maximum cell deformation is not limited by cell thickness or substrate stiffness. In order to explore possible mechanisms of cell force response,

* Corresponding author. Tel.: +1 217 333 8552; fax: +1 217 244 6534.
E-mail address: saif@uiuc.edu (M. Taher A. Saif).

1742-7061/$ - see front matter © 2006 Acta Materialia Inc. Published by Elsevier Ltd. All rights reserved.
doi:10.1016/j.actbio.2006.07.005

we employed the green fluorescent protein (GFP) technique to visualize the evolution of the actin network during indentation. We found a direct correlation between the measured force response and the adaptive transformation of actin network. These results shed new light on how cells sense and respond to mechanical stimuli, particularly injuries.

2. Materials and methods

2.1. Force sensors

Fig. 1A shows a two-component force sensor, which consists of a flexible sensor beam, a rigid bar, a sensor probe attached to the free end of the rigid bar, and a measurement reference bar attached to the sensor base. The probe can be designed according to the desired contact configuration between the probe and cells. Fig. 1C shows the scanning electron microscopy (SEM) micrograph of a two-component force sensor. Here, the lengths of the sensor beam and rigid bar were $L_1 = 1$ mm and $L_2 = 0.429$ mm, respectively. The cross section of the sensor beam was 2.0 μm (in plane of paper) × 13.1 μm (normal to the plane). The rectangular shape and dimensions (about 2 μm × 5 μm) of the probe are illustrated in the upper right box of Fig. 1A. The depth of the probe was 13.1 μm. The sensor was made of single crystal silicon by the process described in Ref. [11]. An $x - y - z$ piezo actuator was

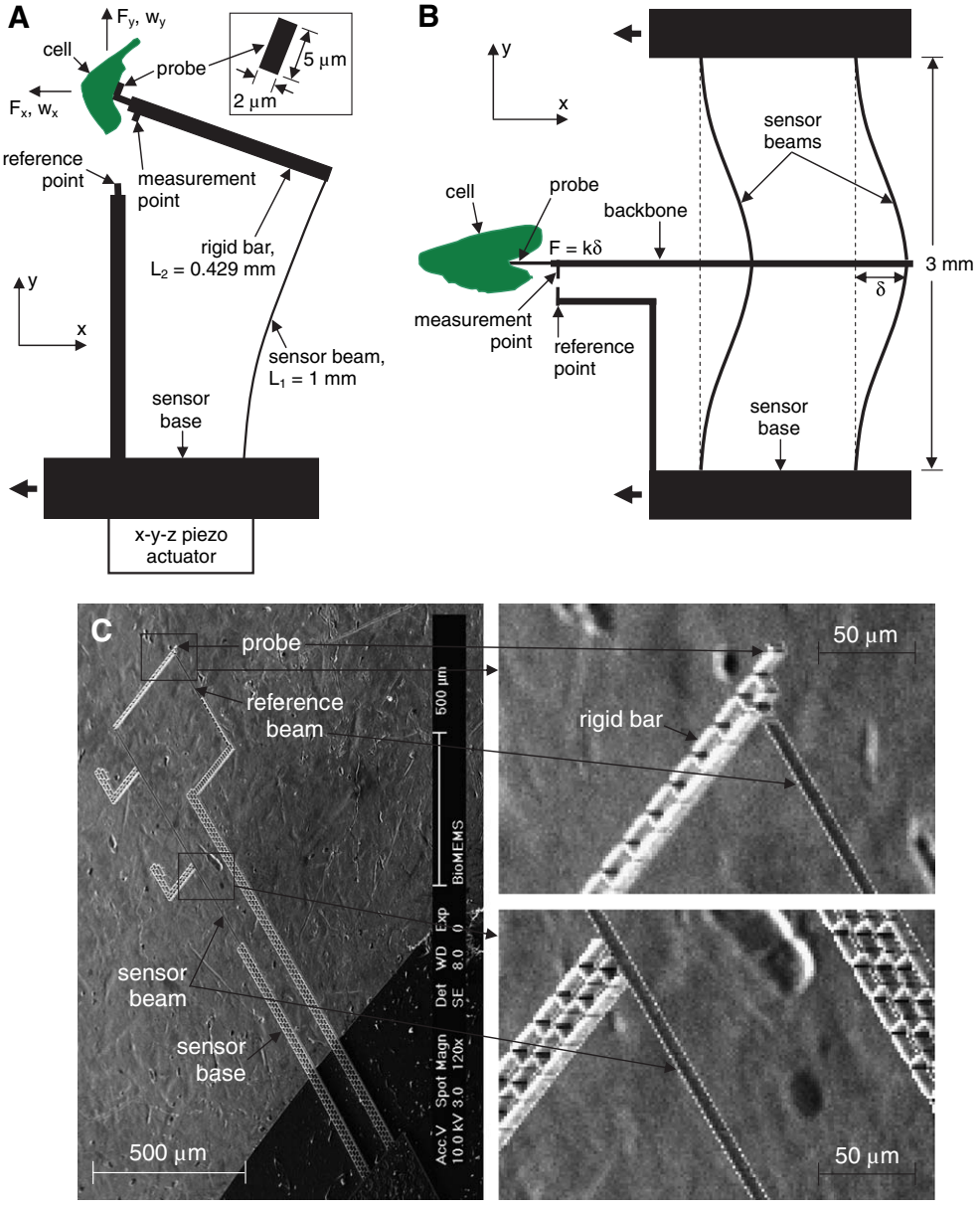

Fig. 1. (A) Schematic drawing of a two-component MEMS force sensor. (B) Schematic drawing of a single-component MEMS force sensor. In (A) and (B) the sensor probe is about 1–2 μm over the surface of the substrate on which the cells are cultured. (C) Scanning electron microscope images of the two-component force sensor and the zoom in views for the probe and sensor beam, respectively.

Please cite this article as: Shengyuan Yang, M. Taher A. Saif, Force response and actin remodeling (agglomeration) in fibroblasts ..., Acta Biomaterialia (2006), doi:10.1016/j.actbio.2006.07.005

used to move the sensor base along the $-x$ direction to laterally indent the cells (Fig. 1A).

Two sets of data were recorded during indentation: deformation of the cell and the corresponding force response. Cell deformations in the x and y directions, denoted by D_x and D_y, respectively, at the point of contact between the cell and the probe were measured from the movement of the sensor probe (since the sensor probe was always in contact with the cell). The force exerted by the cell on the probe is estimated from the sensor deflections, w_x and w_y, measured from the relative displacements between the measurement point and the reference point. The two components of the force, F_x and F_y, were obtained from

$$\begin{bmatrix} F_x \\ F_y \end{bmatrix} = \frac{2EI}{L_1^3} \begin{bmatrix} 6 & 3\frac{L_1}{L_2} \\ 3\frac{L_1}{L_2} & 2\left(\frac{L_1}{L_2}\right)^2 \end{bmatrix} \begin{bmatrix} w_x \\ w_y \end{bmatrix}, \quad (1)$$

where $E = 170$ GPa is the Young's modulus and I is the moment of inertia of the sensor beam. If, for example, $w_x = 1$ μm, $w_y = 0.5$ μm, from Eq. (1), we get $F_x = 28.2$ nN, $F_y = 36.9$ nN. The magnitudes of the cell deformation and force response are $\sqrt{D_x^2 + D_y^2}$ and $\sqrt{F_x^2 + F_y^2}$, respectively. The cell deformation in the x direction is considered negative when the cell is under indentation. The cell deformation in the y direction is positive when the cell is deformed upward (see for example Fig. 1A). Cell deformation, sensor deflection and force response are measured with respect to the initial indentation state (after initial observation of the cell for 20 min under a small indentation; see Section 3).

A single-component force sensor was used for indentation while visualizing the actin network by tagging with GFP. The schematic of such a sensor is shown in Fig. 1B. It has two parallel beams that measure the force response. The sensor applies indentation and measures cell force response only along the x direction. The sensor beams were 3 mm long with 2.1 μm × 7.7 μm in cross section, which results in a sensor stiffness of 14.4 nN/μm. The width and depth of the sensor probe were also 2.1 μm and 7.7 μm, respectively.

2.2. Cell culture and force response measurement

The cells were cultured from a monkey kidney fibroblast (MKF) cell line (CV-1, ATCC, Manassas, VA). They were cultured in a medium with 90% DMEM (ATCC, Manassas, VA) and 10% FBS (ATCC, Manassas, VA) in an environment with 37 °C temperature and 5% CO_2. For in situ visualization of actin during force response measurement, the cells were transfected with the pEGFP-Actin vector (BD Biosciences Clontech, Palo Alto, CA) by using CLONfectin (BD Biosciences Clontech, Palo Alto, CA). The force response measurement was conducted in air at room temperature after 60 h of transfection. An inverted optical microscope (Olympus IX81, Olympus America, Melville, NY) with an objective of 20× was used to image the cell deformations and sensor deflections. A cooled charge-coupled device camera (MagnaFire S99806, Olympus America, Melville, NY) and its corresponding data acquisition software were used with the microscope to collect the images and measure the data. The entire experimental system has been described in detail in Ref. [11]. The force resolution of the measurement system using the two-component force sensor was estimated to be 0.6 nN by multiplying the displacement measurement resolution, 0.14 μm, with the spring constant of the sensor beam in the x direction. Each indentation step was taken within 1 s by moving the sensor base with the piezo actuator. The cell deformation and force response were recorded 15 s after each indentation step. The time delay between two consecutive indentation steps was kept at 50 s unless otherwise stated. In order to contact a cell, the sensor probe was first lowered to gently contact the bottom of the Petri dish on which the cells were cultured. The probe was then lifted up by about 1–2 μm, and moved laterally to contact and indent a well-spread and attached cell by a few micrometers. The initial indentation established a stable (non-sliding) contact configuration between the front surface of the probe and the cells. The cell was then observed for the next 20 min for any shape change and movement. The cells that did not undergo any apparent morphological change/migration were considered for force response study.

3. Results and discussion

3.1. Loading and unloading force response

Fig. 2 shows a typical force response of an MKF subject to large lateral indentation by the two-component force sensor and three phase contrast images during indentation. Fig. 2A shows the magnitude of the cell force response resultant, $\sqrt{F_x^2 + F_y^2}$, versus the magnitude of the cell deformation resultant, $\sqrt{D_x^2 + D_y^2}$; Fig. 2B shows the cell deformation components, D_x and D_y; Fig. 2C shows the cell force components, F_x and F_y. The rest of the panels show the phase contrast images at different cell deformation states.

Fig. 2A shows that the force response is linear until the cell indentation reaches about 35 μm (a–c), which is comparable to the cell size, followed by plastic yielding which is possibly triggered by significant damage of the cell cytoskeletal structure (from c to d). We will show later that remodeling of the actin network occurs during this yielding process, which is an adaptive biological response, different from the mechanical one. Such plastic yielding was not observed under large stretches [10]. At the beginning of the unloading process, the force response dropped sharply (d–e). Two linear responses (e–f and f–g) followed with further unloading. Thus the force response was strongly hysteretic.

Please cite this article as: Shengyuan Yang, M. Taher A. Saif, Force response and actin remodeling (agglomeration) in fibroblasts ..., Acta Biomaterialia (2006), doi:10.1016/j.actbio.2006.07.005

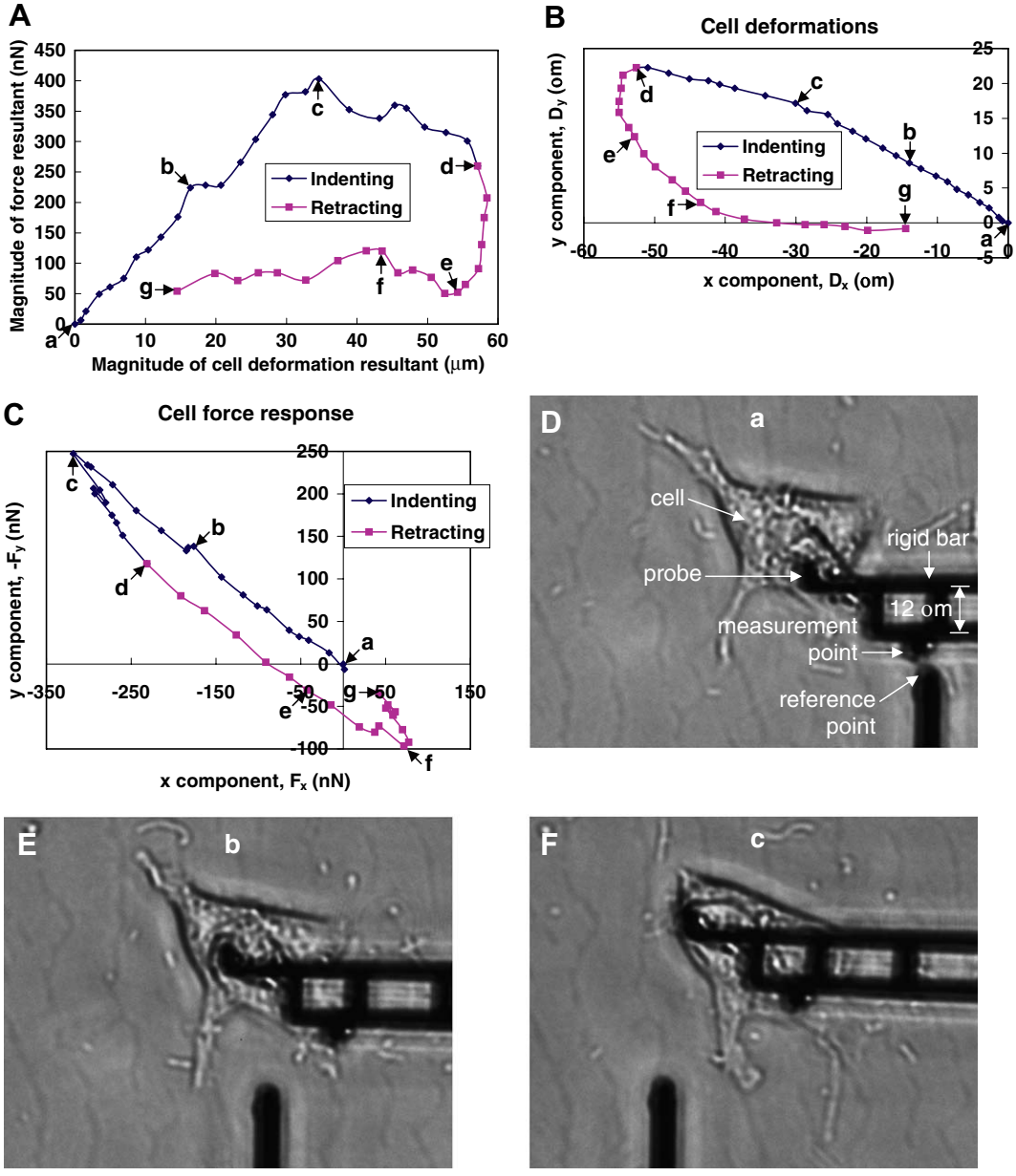

Fig. 2. Results for a widely spreaded monkey kidney fibroblast obtained by the two-component force sensor. (A) Magnitude of cell force response versus magnitude of cell deformation. (B) Cell deformations in the x and y directions. (C) Cell force response in the x and y directions. (D)–(F) Phase contrast images at the cell deformation states specified in (A)–(C).

Fig. 2B and C show that as the cell was deformed between a and c, the directions of the deformation and the force response remained the same (straight line between a and c). But the resistance of the cell against deformation (i.e., the cell stiffness) in the y direction was higher than that in the x direction. Hence the angle between the deformation vector (a–c) and $-x$ axis was 30.8°, whereas the angle between the force response vector (a–c) and $-x$ axis was 37.1°. This result shows that the structural anisotropy revealed by the magnetic twisting cytometry for human airway smooth muscle cells [12], where the induced surface deformation of the cells was ~0.2–0.6 μm, may be applicable to a deformation range of about two orders of magnitude higher. Fig. 2B also shows that cell deformation is irreversible, as the loading and unloading paths were different.

The linear response during the first phase of indentation (Fig. 2A) is surprising, as it differs from some earlier reports. For example, non-linear (stiffening) cell force response was observed under indentation by cell poker technique [13] and AFM [14–16], as well as under compression by a pair of microplates [17]. Note that, in all these experiments, cell deformations were orthogonal to the substrate, and were small, limited by cell thickness. The tensegrity cell structural model predicts a cell stiffening force response [2,18,19]. Non-linear mechanical behavior of biological soft tissues is also well-established [4,20,21]. We believe that the linear force response observed in this study

Please cite this article as: Shengyuan Yang, M. Taher A. Saif, Force response and actin remodeling (agglomeration) in fibroblasts ..., Acta Biomaterialia (2006), doi:10.1016/j.actbio.2006.07.005

under large lateral indentations may arise due to biological adaptation of the cell, i.e., the cell response is both mechanical and biological. The observed remodeling of the actin network (see next section) reveals a dramatic biological response under sustained indentation. In order to explore the time dependence of such a biological response, we carried out an indentation experiment over a time span of 1.7 s (Fig. 3), in contrast to 37.5 min (Fig. 2). We again found a linear force response, with small initial non-linearity. Thus, if the linear response is due to biological adaptation, it must take place within a time scale much shorter than a second.

We also note that, during indentation, although the cells adhere on the substrate, local actin network may be partially damaged and some of the cell attachments with the substrate may unbind due to the invasion of the sensor probe. Either of these mechanisms will cause mechanical softening, which, together with expected mechanical stiffening during indentation, may result in an apparent linear response. However, Figs. 2 and 4 suggest that local damage of actin network compared to the overall network and local unbindings compared to the overall span of attachments are small. Hence their influence on the overall force response is expected to be small.

3.2. Remodeling of actin network

In order to explore the underlying mechanism of the force response, we observed the deformation of the actin filaments in transfected MKFs during indentation force response measurement by the single-component force sensor (Fig. 1B). Fig. 4A shows the force response of an MKF. The response shows initial non-linearity, an intermediate linear regime, and a long plastic regime. Fig. 4C–H shows the representative fluorescent images at times indicated. Due to photobleaching, the relative brightness corresponding to the actin in these images decreased with increasing observation time, but the distribution of the actin can still be clearly seen. Panels C and D are in the initial non-linear/linear force response regime where deformation of the actin is highly localized, i.e., only the actins on the way of the probe and its nearby region are deformed, but there is no significant deformation far away from the probe. Panels E–H are in the plastic response regime where part of the actin network far away from the probe lose distinct features and form well-defined circular structures. The higher brightness of these circular structures indicates that these regions are actin agglomerates. With increasing time, the agglomerates grow in size but not in numbers, and a slight relaxation in the force response is observed.

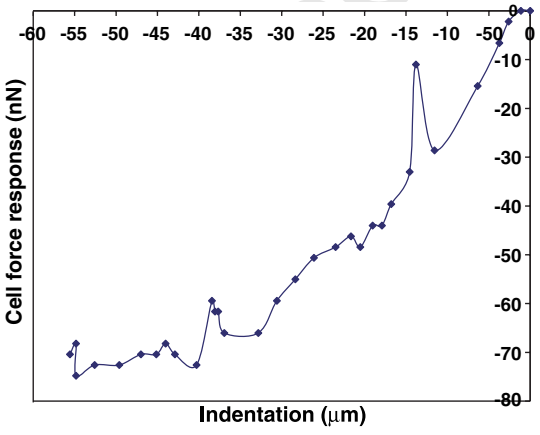

Fig. 3. Fast indentation force response of a monkey kidney fibroblast obtained by the single-component force sensor. The time span for the entire experiment is 1.7 s, compared to 37.5 min in Fig. 2.

Fig. 5 shows agglomeration in three MKFs during and after indentation with a probe and a plate. In Fig. 5A, the agglomerates continued to increase in size even after the probe is withdrawn, and the actin network did not reappear implying that the process of actin remodeling is irreversible. These observations suggest that large sustained indentation or compression induce decomposition of the stress fibers and reorganization of the decomposed stress fibers into well-defined agglomerates in the cell. In Fig. 5B, a plate was used to compress a cell instead of indenting it by a probe. Such compression avoids possible local damage of cell membrane by a probe. The observation of actin agglomeration implies that such remodeling is possibly a general response of a cell under compression or indentation. Fig. 5B also shows local unbinding of the actin network may occur even far away from the region of compression. Fig. 5C shows agglomeration in a cell that is indented and the cell membrane is punctured.

3.3. Observations and interpretations

3.3.1. Size and distribution pattern of agglomerates

Although agglomerates appear all over the cell, they are located at discrete locations only. These agglomerates are mostly circular and hence are likely to occupy spherical or penny shaped domains (constrained by cell membrane, Fig. 5A, middle panel). The fluorescent intensity over most of their size is similar to or higher than the pre-existing actin network (where the agglomerates are formed). This suggests that the agglomerate is formed by actin contributed not only by the actin network it might have replaced but also by other resources as well.

3.3.2. Spatial pattern of agglomerates

Figs. 4 and 5 show that the spatial distribution of actin agglomerates follow the actin fiber distribution pattern in the pre-indented cell. These agglomerates appear and grow simultaneously. During the initial phase of growth, they appear to be away from the basal cell membrane (on the substrate) and closer to the apical (top) cell membrane, which is noticed by focusing at the plane of the substrate and above. As the agglomerates increase their size, they become bounded by the top and bottom membranes as seen from the phase contrast image (Fig. 5A, middle

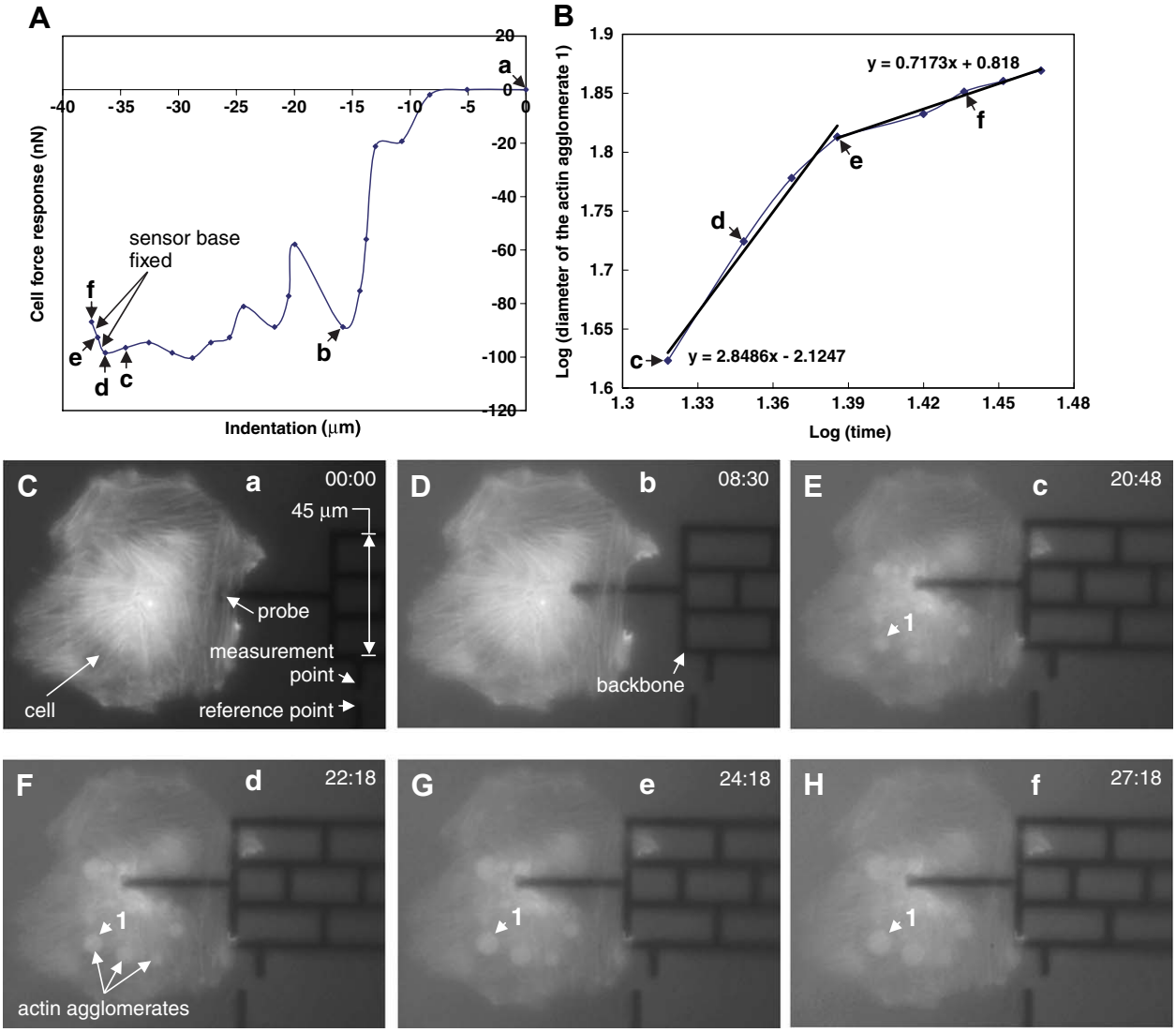

Fig. 4. Results for a GFP-actin transfected monkey kidney fibroblast (MKF). (A) Indentation force response obtained by the single-component force sensor. (B) Logarithm of the diameter of the circular actin agglomerate 1 (formed in the cell and indicated in (E)–(H)) versus logarithm of the time. The diameter of the agglomerate is in the units of image pixel and the time is in units of minutes. (C)–(H) Representative fluorescent images during the measurement at the cell deformation states specified in (A) (min:s). (C) The MKF before the indentation. (G) and (H) were recorded 2 and 5 min after (F), respectively, with the sensor base fixed.

panel). In Fig. 5C, where the cell membrane is punctured, agglomeration is neither simultaneous nor are the agglomerates distributed all over the cell. Their distribution is initially localized near the injured region. With time, they begin to appear in regions away from the injury. We will return to this observation to develop a hypothesis on the agglomeration mechanism.

Prior to indentation, the fibers were straight, stable (no apparent thermal fluctuation) and long, on the order of 30 μm or higher. Since the persistence length of single actin fibers is about 18 μm [22], the long straight in vivo fibers suggest that they were under tension and/or each fiber consisted of many single fibers. Absence of fibers along orthogonal directions (i.e., fibers along one direction only, Figs. 4 and 5) suggests that most of the regional intracellular forces were along the direction of the fiber alignment. The alignment of agglomerates along the direction of fibers and their simultaneous growth (in cells where cell membrane is not punctured, Figs. 4 and 5A and B) suggest that they were initiated at points where stress change was high under indentation. Also, Fig. 5C shows voids and cracks in the actin network that developed during indentation between parallel fibers suggesting that forces orthogonal to the fiber direction develop which separate them from one another laterally.

3.3.3. Cell viability

In order to test whether the cells were alive after formation of agglomerates, we applied 0.4% trypan blue solution (Sigma–Aldrich, St. Louis, MO) in the cell medium after the indentation experiment. We found that the cells with agglomerates became blue indicating that they were dead.

Please cite this article as: Shengyuan Yang, M. Taher A. Saif, Force response and actin remodeling (agglomeration) in fibroblasts ..., Acta Biomaterialia (2006), doi:10.1016/j.actbio.2006.07.005

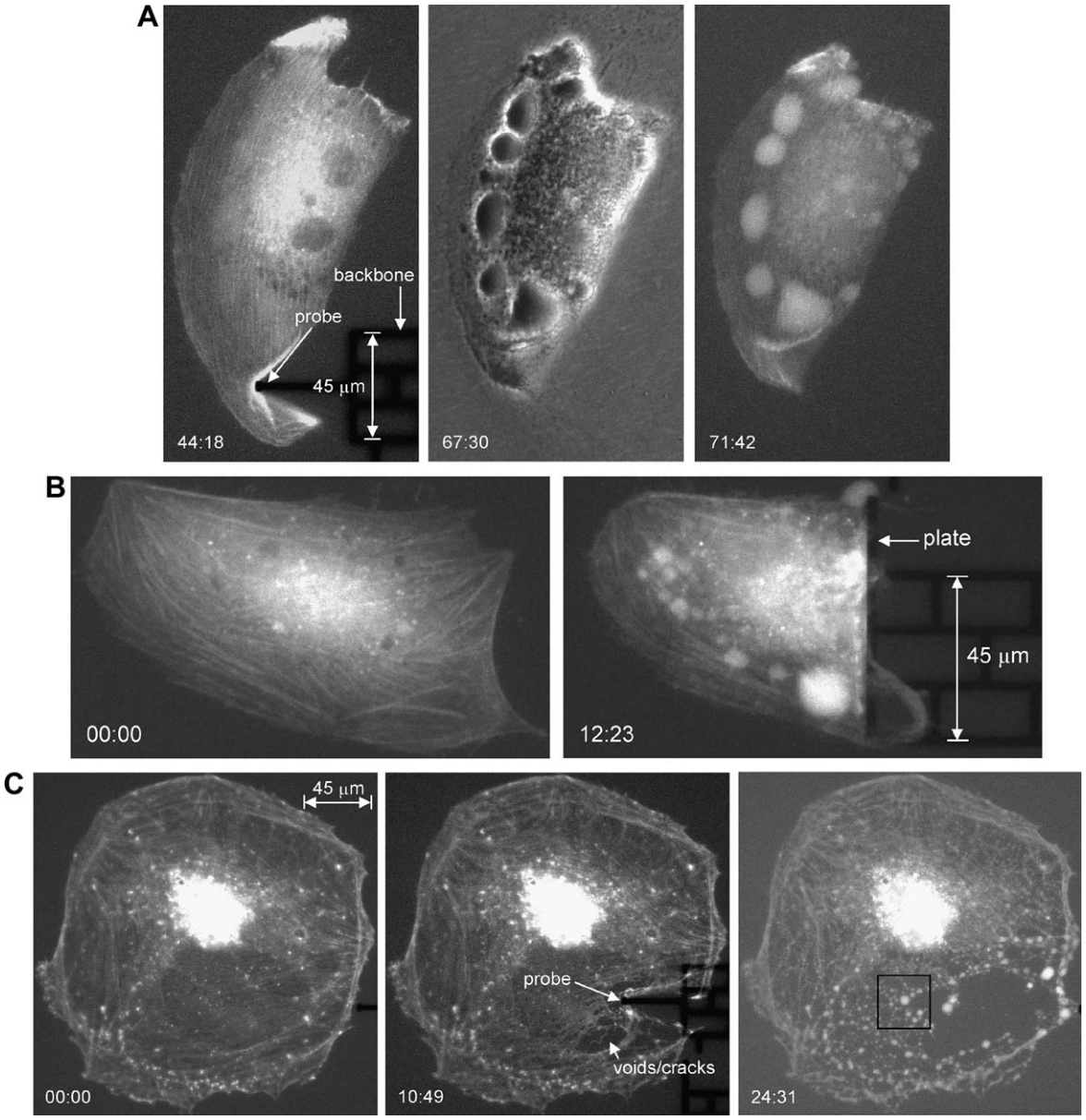

Fig. 5. (A) Response of the actin network in a GFP-actin transfected monkey kidney fibroblast due to the probe indentation and retraction (the middle panel is a phase contrast image). (B) Response of the actin network in a GFP-actin transfected monkey kidney fibroblast due to a plate compression. (C) Response of the actin network in a GFP-actin transfected monkey kidney fibroblast due to the probe indentation and retraction, where the cell membrane is punctured (min:s).

Thus, agglomeration might be the pre-apoptotic state of the cell induced by mechanical indentation.

3.3.4. Time to agglomeration

We indented a cell by about 32 μm, and held the indentation fixed until agglomeration could be detected. We found that the time to agglomeration was about 1 min. It thus appears that sustained indentation beyond a threshold value initiates agglomeration.

3.3.5. Agglomeration in untagged cells

Actin agglomerates appeared as blebs in the phase contrast image of the cell (Fig. 5A, middle panel). In order to test whether agglomeration dynamics under indentation is an artifact of GFP tagging of actin, we indented cells without florescent tags. Blebs appeared in these cells as well under indentation, implying that agglomeration is a general response to mechanical probing unaffected by tagging.

3.4. Agglomeration kinetics

Fig. 4B shows the time dependence of the diameter of the actin agglomerate 1, indicated in Fig. 4E–H, plotted on a log–log scale. Here, the diameter of the agglomerate is in the units of pixel (of the images) and the time is in the units of minutes. The dependence shows two distinct

Please cite this article as: Shengyuan Yang, M. Taher A. Saif, Force response and actin remodeling (agglomeration) in fibroblasts ..., Acta Biomaterialia (2006), doi:10.1016/j.actbio.2006.07.005

regions, i.e., the initial region with a slope of 2.85 and the remaining region with a slope of 0.72, i.e., initially the agglomerates grow at a fast rate with time as $t^{2.85}$, followed by a slow rate of $t^{0.72}$, where t is the time. Note that, due to photobleaching, the growth can be measured only for a limited time. Hence, such transition of growth rates may not be traced unless it occurs before photobleaching.

In order to form a statistics of growth rates, we determined the exponents (α) for 18 such agglomerates from cells that did not undergo any observable shrinkage or expansion while the agglomerates were growing. Such size change would influence the diameter change of the agglomerates. Fig. 6A shows the histogram of growth exponents. Note that a few agglomerates contributed two exponents, a high and a low one representing two growth rates if they appeared before photo-bleaching. The statistics show two peaks in the vicinity of $\alpha = 0.5$ and 2.5.

3.4.1. Interpretation of the faster growth rates

The higher exponents ($\alpha = 2$–3) suggest a non-diffusive mechanism. The fast growth cannot be explained by decomposition of the pre-existing actin network spanned by the domain of the agglomerate alone. For then the intensity of the agglomerate would be significantly lower than the initial actin fibers contributing to the agglomerate.

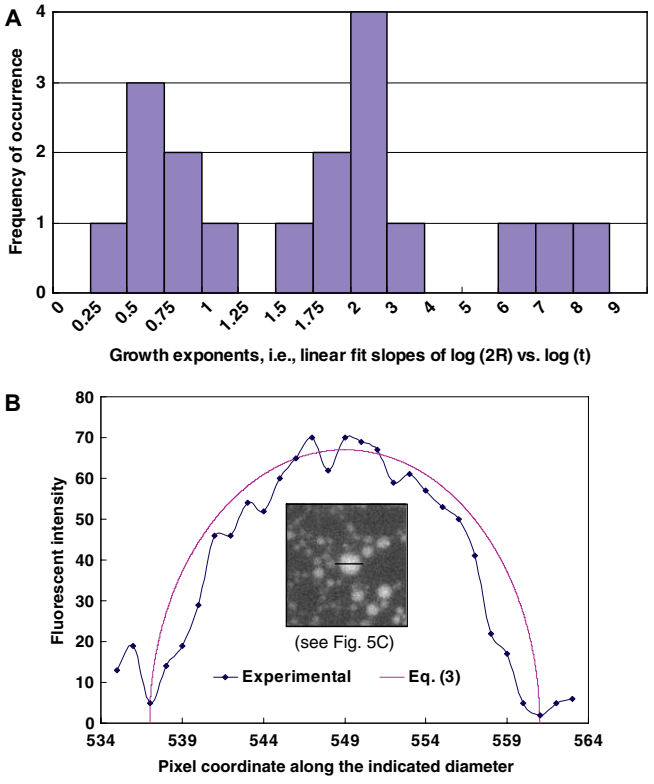

Fig. 6. (A) Histogram of growth exponents of 18 agglomerates formed in the actin network in GFP-actin transfected monkey kidney fibroblasts. (B) Fluorescent intensity profile (the experimental curve) in gray scale units along the diameter of an actin agglomerate shown in Fig. 5C. The predicted intensity profile by Eq. (3) is also shown, where C_0 and Dt are chosen such that the predicted and experimental peaks match.

The actin, initially constrained within the fibers, would have to occupy a much bigger volume thus lowering the concentration and the corresponding intensity. Experimentally, we see the reverse. The increased amount of actin within the agglomerate is probably contributed by actin monomers available in the cytoplasm generated by uncoupling of sequestering molecules. A possible mechanism of agglomerate dynamics is discussed later.

3.4.2. Interpretation of the slower growth rates

The lower growth rate ($\alpha = 0.5$–1) suggests a diffusive mechanism, i.e., once the actin fibers decompose at a region, and if there is no addition of actin, then the accumulated actin diffuses outward. If the diffusing species satisfies the Fick's law of diffusion, then its concentration, C, is governed by

$$\frac{\partial C}{\partial t} = D\nabla^2 C, \text{ and } C \text{ evolves with time as } C = \frac{C_0}{(Dt)^{\frac{3}{2}}} e^{-\frac{r^2}{4Dt}} \quad (2)$$

where D is the diffusion constant, r is the distance from the center of the diffusing agglomerate, and C_0 is a constant. If the radius of the agglomerate is characterized by R where $C(R) = C^* \ll$ peak concentration at any $t > 0$, then from Eq. (2), $R \sim t^{\frac{1}{2}}$, i.e., $\alpha = 0.5$, similar to the exponent obtained experimentally. Hence the slow growth rate is most likely determined by diffusion. We further note that the brightness at any point of the two-dimensional (2D) image of an agglomerate is contributed by the accumulated florescence over the depth of the sphere (if the agglomerate is spherical). Thus the brightness intensity, $I(x)$, at any point x from the center is given by

$$\begin{aligned} I(x) &= 2\int_0^{\sqrt{R^2-x^2}} C(r)\mathrm{d}y \\ &= 2\int_0^{\cos^{-1}\frac{x}{R}} C\left(\frac{x}{\cos\theta}\right)x(1+\tan^2\theta)\mathrm{d}\theta \\ &= \frac{2C_0 x}{(Dt)^{\frac{3}{2}}}\int_0^{\cos^{-1}\frac{x}{R}} (1+\tan^2\theta)e^{-}\frac{x^2}{4Dt\cos^2\theta}\mathrm{d}\theta, \end{aligned} \quad (3)$$

where x is the distance from the center of the agglomerate (2D image).

Fig. 6B shows the 2D image (inset) of an agglomerate that grows with time as t^{α} with $\alpha = 0.93$, and its intensity profile (the experimental curve in Fig. 6B is obtained by the image analysis software Scion Image [23]) in gray scale units along the diameter. Also plotted in the figure is the predicted intensity profile $I(x)$ along the diameter using Eq. (3). Here, C_0 and Dt are chosen such that the predicted and experimental peaks match. The close match between the experimental and theoretical intensity profiles point to a diffusive spreading of the agglomerate.

Note, however, that the diffusion time of the actin monomer to travel across the cell (tens of micrometers) is on the order of a second [24]. Since the mean square dis-

placement, $\langle r^2(t)\rangle$, of a diffusing species is given by, $\langle r^2(t)\rangle = 2Dt$, we get $D \sim 50\ \mu m^2/s$ for $\langle r^2\rangle \sim 100\ \mu m^2$ and $t \sim 1$ s. If the species within the agglomerate were actin monomers with $D \sim 50\ \mu m^2/s$, then they would diffuse out within 10 s, and the fluorescent intensity would decrease by two orders of magnitude by then. Since the agglomerates, some of which appear to be isolated from the rest of the actin network, grow over a time span of several minutes, it implies that the diffusion coefficient (if diffusion is the mechanism of spreading) of actin species within the agglomerates is a few orders of magnitude less than that of actin monomer. This suggests that the agglomerates consist of species that are much larger than monomers (e.g., segments of actin fibers), or they may have mutually attractive interaction between them which retards spreading.

3.5. Hypothesis on actin agglomeration

3.5.1. Agglomeration is initiated by indentation/compression and triggered by the increase of the intracellular Ca^{2+} content

Actin agglomeration observed here is possibly triggered by the increase of the intracellular Ca^{2+} content. Ca^{2+} could be released from intracellular storage vesicles, a process stimulated by IP3, and IP3 could be generated by mechanically (here it is the mechanical indentation/compression) induced activation of phospholipase C [25]. The time for intracellular Ca^{2+} to increase may be only 60 s [26], similar to the time to initiate actin agglomeration (about 1 min, see above) under sustained indentation. Another possibility for the increase of the intracellular Ca^{2+} content is the influx of Ca^{2+} through mechanical force-induced pores on the cell membrane from extracellular space.

Thus, under sustained indentation/compression, Ca^{2+} is released from intracellular sources or introduced from extracellular space through pores at stress high points. The excessive Ca^{2+} may trigger uncoupling of sequestering proteins (such as thymosin) from actin monomers in the cytoplasm [26]. This could generate an abundant supply of actin monomers ready to be polymerized to form actin filaments. The excessive Ca^{2+} also activates gelsolin which severs actin filaments (in the existing actin network and newly formed actin filaments) into actin fragments and caps their plus ends [24]. Thus, the combined effect of activated actin monomers and presence of gelsolin may lead to a local rapid accumulation of actin fragments, which may explain the fast growth rate of agglomerates. The process continues until the local Ca^{2+} concentration decreases to the normal intracellular level. Further spreading of accumulated actin segments is then achieved by diffusion, with a diffusion constant much smaller than that of single actin monomer due to the larger size of actin fragments. Sustained indentation causes sustained release (instead of typical short temporal bursts) of Ca^{2+} which may lead to apoptosis [27].

If the cell membrane is fractured (Fig. 5C), then Ca^{2+} can largely enter the cell from the external medium. The locally increased Ca^{2+} level near the ruptured region triggers the above process causing actin agglomeration. Such agglomeration spreads towards the rest of the cell with time due to the diffusion of extracellular Ca^{2+} towards the interior of the cell, in contrast to the simultaneous formation of agglomerates at the stress high points all over the cell. The overall spatial distribution of the agglomerates due to the fracture of cell membrane appears random, whereas that due to intracellular high stress follows the stress fiber pattern.

4. Remarks

1. Agglomeration of actin is not unusual and has been observed in mice neurons induced by the treatment of cytochalasin D [28], in chicken muscle actin induced by gamma-radiation [29], in the reorganization of depolymerized actin in *Dictyostelium* cells by the treatment of latrunculin A [30], and in proximal tubule cells by ischemic injury [31]. The actin network is found to depolymerize and form agglomerates in the late feeding stage of working larvae, which coincide with the apoptotic wave [32]. We have also observed actin agglomeration in MKFs due to the treatment of trypsin-EDTA (images not shown). To the best of our knowledge, this is the first evidence of actin agglomeration followed by cell death due to local mechanical indentation and damage. It is interesting to note that cells may signal similar processes due to such diverse stimuli as mechanical and biochemical ones.
   It was reported that eupodia, being F-actin-containing cortical structures, are formed locally in invasive locomotion in *Dictyostelium* at the base of a lamellipodium advancing to invade a tight space, and it appears that the mechanical stress at the leading edge modulates the structural integrity of actin and its binding proteins, such that eupodia are formed when anchorage is needed to boost for invasive protrusion of the leading edge [33]. It was also reported that podosomes, being invasive adhesion structures and an F-actin-rich core surrounded by a ring structure containing proteins such as vinculin and talin, are formed locally in transformed fibroblasts by oncogenic Src causing disruption of actin stress fibers [34,35]. Thus, the *Dictyostelium* eupodia and the podosomes are formed to strengthen the adhesion between the cells and substrate and to bear the mechanical force exerted by the cell migrating movement, and of course they should be subjected to this mechanical force during the cell migrating movement. The actin agglomerates we observed here are different. As mentioned in the above, here the depolymerization of stress fibers and agglomeration of actin are initiated at high stress points existing in the actin network induced by sustained indentation, i.e., the mechanical force induces the actin agglomerates. Also, the actin agglomerates do not strengthen the cells

Please cite this article as: Shengyuan Yang, M. Taher A. Saif, Force response and actin remodeling (agglomeration) in fibroblasts ..., Acta Biomaterialia (2006), doi:10.1016/j.actbio.2006.07.005

since the increase in the cell force response was not observed after the agglomerates were formed. There are two other significant differences between the actin agglomeration observed here and the eupodia and podosomes. First, the actin agglomerates grow significantly with time (as shown in the above), whereas the significant growing of eupodia and podosomes was not observed after they were formed. Second, the actin agglomerates do not seem to be attached to or even located close to the intracellular side of the adhering cell surface, whereas eupodia and podosomes are ventral structures. But, depending on the cell types, all these actin assemblies show different types of mechanobiological response of the cells to their mechanical force/stress environments, although maybe initiated and formed by different mechanisms.

Mechanical modifications of the actin network can be mediated also by hyperosmotic stresses. Accumulation of actin filaments along the margin of the *Dictyostelium* cells was observed after the contraction of these cells in response to hyperosmotic stress [36], but actin agglomeration well inside the cells was not observed.

2. The study also reveals a fundamental difference between a living specimen and a non-living one. The former responds both mechanically and biologically when subjected to a mechanical stimulus, whereas the latter responds only mechanically. The biological response is a result of a cascade of events and signals that we have very little knowledge about. When we measure the response, we measure both the mechanical and the biological contributions (such as actin agglomeration far from the point of indentation) with very little detail on how to decouple one from the other. Nature, most likely, engages both. If the mechanical stimulus is small and is over a short time, the biological response may be negligible. The challenge is in reducing the large parameter space of the biological response to a few important ones so that one can formulate a quantitative approach in interpreting the measured combined response.

5. Conclusions

In this paper, the loading and unloading force response of single living fibroblasts due to large lateral indentation has been measured by MEMS force sensors. The actin network of cell cytoskeleton has been observed in situ by using the GFP technique, which reveals how cells adapt to mechanical indentation and injuries by cytoskeletal reorganization, and provides mechanistic interpretation for the measured force response.

We found: (1) The indentation force response is highly irreversible (i.e., hysteretic) in contrast to the observed reversible and repeatable linear cell force response for the case of large local stretch [10]. (2) All the loading processes show linear force response (sometimes with small initial non-linearity) for indentations as large as the size of the cells. Plastic yielding follows on further indentation. (3) Cell mechanical response is anisotropic. (4) Upon sustained indentation, the actin network possibly decomposes irreversibly at discrete locations all over the cell and forms circular agglomerates. (5) The spatial distribution of the agglomerates follow the stress fiber orientation of the pre-indented cell. (6) The size of the agglomerates grows with time initially at a fast rate as t^{α} with $\alpha = 2$–3 followed by a slow rate with $\alpha = 0.5$–1. The transition from fast to slow rates happens abruptly. Actin agglomeration has been observed in living cells subject to ischemic injury, toxic treatment, and at certain developmental stages of larvae, and is believed to be the pre-apoptotic phase of such cells. To the best of our knowledge, this is the first evidence of actin agglomeration due to local mechanical indentation. The finding suggests that living cells, when mechanically indented, injured or compressed, may also initiate actin reorganization and agglomeration with consequent loss of stiffness. In other words, two distinct stimuli, one mechanical and the other biochemical, may result in similar cell signalings. The study may have implications in understanding the role of radial compression on the damage of the endothelium in blood vessels during formation of plaque and progression of atherosclerosis.

Acknowledgements

We thank Professor Roger Kamm of the Massachusetts Institute of Technology and Professor Erich Sackmann of the Technical University of Munich for helpful discussions. This work was supported by the National Science Foundation (NSF) Grants ECS 01-18003 and ECS 05-24675. The MEMS force sensors were fabricated at the Center for Nanoscale Science and Technology at the University of Illinois at Urbana-Champaign.

References

[1] Bao G, Suresh S. Cell and molecular mechanics of biological materials. Nature Mater 2003;2:715–25.
[2] Ingber DE. Tensegrity I. Cell structure and hierarchical systems biology. J Cell Sci 2003;116:1157–73.
[3] Galbraith CG, Sheetz MP. A micromachined device provides a new bend on fibroblast traction forces. Proc Natl Acad Sci USA 1997;94:9114–8.
[4] Hayashi K. Mechanical properties of soft tissues and arterial walls. In: Holzapfel GA, Ogden RW, editors. Biomechanics of soft tissue in cardiovascular systems. New York (NY): Springer; 2003. p. 15–64.
[5] Maurel W, Wu Y, Magnenat Thalmann N, Thalmann D. Biomechanical models for soft tissue simulation. Berlin: Springer-Verlag; 1998.
[6] Nordin M, Lorenz T, Campello M. Biomechanics of tendons and ligaments. In: Nordin M, Frankel VK, editors. Basic biomechanics of the musculoskeletal system. Philadelphia (PA): Lippincott Williams & Wilkins; 2001. p. 102–25.
[7] Pfister BJ, Weihs TP, Betenbaugh M, Bao G. An in vitro uniaxial stretch model for axonal injury. Ann Biomed Eng 2003;31:589–98.

[8] Freyman TM, Yannas IV, Pek Y-S, Yokoo R, Gibson LJ. Micromechanics of fibroblast contraction of a collagen-GAG matrix. Exp Cell Res 2001;269:140–53.
[9] Langer R, Tirrell DA. Designing materials for biology and medicine. Nature 2004;428:487–92.
[10] Yang S, Saif T. Reversible and repeatable linear local cell force response under large stretches. Exp Cell Res 2005;305:42–50.
[11] Yang S, Saif T. Micromachined force sensors for the study of cell mechanics. Rev Sci Instrum 2005;76:Art. No. 044301.
[12] Hu S, Chen J, Fabry B, Numaguchi Y, Gouldstone A, Ingber DE, Fredberg JJ, Butler JP, Wang N. Intracellular stress tomography reveals stress focusing and structural anisotropy in cytoskeleton of living cells. Am J Physiol 2003;285:C1082–90.
[13] Petersen NO, McConnaughey WB, Elson EL. Dependence of locally measured cellular deformability on position on the cell, temperature, and cytochalasin B. Proc Natl Acad Sci USA 1982;79:5327–31.
[14] Alcaraz J, Buscemi L, Grabulosa M, Trepat X, Fabry B, Farre R, Navajas D. Microrheology of human lung epithelial cells measured by atomic force microscopy. Biophys J 2003;84:2071–9.
[15] Touhami A, Nysten B, Dufrene YF. Nanoscale mapping of the elasticity of microbial cells by atomic force microscopy. Langmuir 2003;19:4539–43.
[16] Miyazaki H, Hayashi K. Atomic force microscopic measurement of the mechanical properties of intact endothelial cells in fresh arteries. Med Biol Eng Comput 1999;37:530–6.
[17] Caille N, Thoumine O, Tardy Y, Meister J-J. Contribution of the nucleus to the mechanical properties of endothelial cells. J Biomech 2002;35:177–87.
[18] Coughlin MF, Stamenovic D. A tensegrity model of the cytoskeleton in spread and round cells. ASME J Biomech Eng 1998;120:770–7.
[19] Wang N, Butler JP, Ingber DE. Mechanotransduction across the cell surface and through the cytoskeleton. Science 1993;260:1124–7.
[20] Humphrey JD. Continuum biomechanics of soft biological tissues. Proc R Soc Lond A 2003;459:3–46.
[21] Rubin MB, Bodner SR. A three-dimensional nonlinear model for dissipative response of soft tissue. Int J Solids Struct 2002;39:5081–99.
[22] Gittes F, Mickey B, Nettleton J, Howard J. Flexural rigidity of microtubules and actin filaments measured from thermal fluctuations in shape. J Cell Biol 1993;120:923–34.
[23] Scion Image (Scion Corporation, Frederick, MD).
[24] Alberts B, Johnson A, Lewis J, Raff M, Roberts K, Walter P. Molecular biology of the cell. New York (NY): Garland Science; 2002.
[25] Han O, Takei T, Basson M, Sumpio BE. Translocation of PKC isoforms in bovine aortic smooth muscle cells exposed to strain. J Cell Biochem 2001;80:367–72.
[26] Feneberg W, Aepfelbacher M, Sackmann E. Microviscoelasticity of the apical cell surface of human umbilical vein endothelial cells (HUVEC) within confluent monolayers. Biophys J 2004;87:1338–50.
[27] Berridge MJ, Bootman MD, Lipp P. Calcium – a life and death signal. Nature 1998;395:645–8.
[28] Sattler R, Xiong Z, Lu W-Y, MacDonald JF, Tymianski M. Distinct roles of synaptic and extrasynaptic NMDA receptors in excitotoxicity. J Neurosci 2000;20:22–33.
[29] Niciforovic A, Radojcic MB, Milosavljevic BH. Gamma-radiation induced agglomeration of chicken muscle myosin and actin. J Serb Chem Soc 2004;69:999–1004.
[30] Gerisch G, Bretschneider T, Muller-Taubenberger A, Simmeth E, Ecke M, Diez S, Anderson K. Mobile actin clusters and traveling waves in cells recovering from actin depolymerization. Biophys J 2004;87:3493–503.
[31] Ashworth SL, Southgate EL, Sandoval RM, Meberg PJ, Bamburg JR, Molitoris BA. ADF/cofilin mediates actin cytoskeletal alterations in LLC-PK cells during ATP depletion. Am J Physiol Renal Physiol 2003;284:F852–62.
[32] Schmidt Capella IC, Hartfelder K. Juvenile-hormone-dependent interaction of actin and spectrin is crucial for polymorphic differentiation of the larval honey bee ovary. Cell Tissue Res 2002;307:265–72.
[33] Fukui Y, de Hostos E, Yumura S, Kitanishi-Yumura T, Inoue S. Architectural dynamics of F-actin in eupodia suggests their role in invasive locomotion in Dictyostelium. Exp Cell Res 1999;249:33–45.
[34] Linder S, Aepfelbacher M. Podosomes: adhesion hot-spots of invasive cells. Trends Cell Biol 2003;13:376–85.
[35] Berdeaux RL, Diaz B, Kim L, Martin GS. Active Rho is localized to podosomes induced by oncogenic Src and is required for their assembly and function. J Cell Biol 2004;166:317–23.
[36] Aizawa H, Katadae M, Maruya M, Sameshima M, Murakami-Murofushi K, Yahara I. Hyperosmotic stress-induced reorganization of actin bundles in Dictyostelium cells over-expressing cofilin. Genes Cell 1999;4:311–24.

Please cite this article as: Shengyuan Yang, M. Taher A. Saif, Force response and actin remodeling (agglomeration) in fibroblasts ..., Acta Biomaterialia (2006), doi:10.1016/j.actbio.2006.07.005